International Journal of Reliability, Risk and Safety: Theory and Application

Online ISSN: 2676-3346

Vol. 8/ Issue 2/ 2025/ pp.117-128
DOI: 10.22034/IJRRS.2025.8.2.11
Received: 20 September 2025, Revised: 07 December2025, Accepted: 08 December 2025
Available online at: https://www.ijrrs.com

Original Research Article

Performability Analysis on Two Types of Fixed Structure and Morphed Wings

Iman Shafieenejad *, Ali Mozaffari[2], and Amir Davood Hajjarzadeh[2]

1. Aerospace Research Institute, Ministry of Science, Research, and Technology, Tehran, Iran

2. Faculty of Aerospace Engineering, K. N. Toosi University of Technology, Tehran, Iran

*** Shafieenejad@ari.ac.ir**

Abstract

In this research, a novel computational intelligence-based approach is presented for modeling and predicting the aerodynamic performance of a fish-skeleton-inspired morphing wing. The primary objective is to develop an accurate and efficient model for estimating key aerodynamic parameters, namely the lift coefficient (C_L) and drag coefficient (C_D), based on structural and environmental inputs. To this end, the Adaptive Neuro-Fuzzy Inference System (ANFIS) is utilized due to its high capability in modeling complex and nonlinear systems. The main novelty of this research lies in the implementation and comparative analysis of two distinct ANFIS architectures: an independent model, where two separate ANFIS networks are trained in parallel to predict each output (C_L and C_D), and a dependent (cascaded) model, in which the predicted output from the first network is utilized as an additional input to the second network for predicting the second output. The performance evaluation results, conducted using simulation data and precise statistical metrics, indicate that the independent architecture provides significantly superior prediction accuracy and stability compared to the dependent model. The cascaded approach, despite its theoretical appeal, failed due to the destructive phenomenon of error propagation. Owing to its consideration of the physical dependency between the output parameters. This research not only demonstrates the high efficiency of ANFIS in the field of bio-inspired aerospace structure design but also provides significant insight into the impact of model architecture selection on prediction accuracy and efficiency in multi-input multi-output problems.

Keywords: Morphing Wing; Neuro-Fuzzy System; Bio-inspired Design; Aerodynamic Modeling; Independent Architecture; Dependent (Cascaded) Architecture; Computational Intelligence.

Nomenclature

For clarity and ease of reference, the main symbols and acronyms used extensively in this study are defined below. The lists are arranged in alphabetical order.

ANFIS	Adaptive Neuro-Fuzzy Inference System
CFD	Computational Fluid Dynamics
FIS	Fuzzy Inference System
MIMO	Multi-Input, Multi-Output
RMSE	Root Mean Squared Error
c_i	Center of the i-th membership function (premise parameter)
σ_i	Width of the i-th membership function (premise parameter)
w_i	Firing strength of the i-th fuzzy rule
x , y	Primary continuous input variables
z , C_L	Lift coefficient, the first aerodynamic output
v , C_D	Drag coefficient, the second aerodynamic output
p_i, q_i, r_i	Consequent parameters for the i-th rule in a Takagi-Sugeno model
u_1, u_2, u_3	Discrete control input parameters representing system states

1. Instructions

In the present era, the aerospace industry faces numerous challenges, including the need for increased fuel efficiency, emissions reduction, improved stability, and

How to cite this article:
I. Shafieenejad, A. Mozaffari, and A.D. Hajjarzadeh, "Performability analysis on two types of fixed structure and morphed wings," *International Journal of Reliability, Risk and Safety: Theory and Application*, vol. 8, no. 2, pp. 117-128, 2025, doi: 10.22034/IJRRS.2025.8.2.11.

enhanced flight performance. These challenges have driven researchers and designers the develop technologies capable of addressing the novel and complex demands of modern flight. One of the innovative and transformative approaches in this field is the utilization of adaptive and intelligent structures that can optimize their geometric and functional characteristics under various flight conditions. Among these, morphing wings have emerged as one of the most significant achievements in this domain [1]. By changing their shape in-flight, these wings enable adaptation to varying aerodynamic conditions. They can simultaneously achieve multiple objectives, such as increasing the lift coefficient, reducing drag, improving controllability, and decreasing fuel consumption [2].

In the quest for efficient and adaptive structures, drawing inspiration from biological systems has emerged as a novel and effective approach in the design of advanced aerospace structures. Over millions of years of evolution, nature has provided unique solutions to complex mechanical and structural problems that can inspire engineers in developing new technologies. A prominent example of this inspiration is the skeletal structure of fish, which, with features such as high flexibility, local shape control, and uniform force distribution along the body, serves as an inspiring model for the development of morphing wings. These structures allow fish to execute continuous, controlled, and flow-adaptive movements in variable fluid environments while simultaneously maintaining both strength and flexibility in their bodies [3]. Transferring these characteristics to aircraft wing design can lead to the development of structures that possess low weight, local morphing capabilities, and a rapid response to aerodynamic stimuli [4].

In this context, wing morphing technology has garnered attention as an advanced approach to enhance the aerodynamic characteristics and improve the flight adaptability of modern aircraft [5]. Wing morphing is categorized into three main types: in-plane morphing (span and chord changes), airfoil morphing (thickness and camber changes), and out-of-plane morphing (twist and bend [6]. This research utilizes airfoil morphing technology to significantly enhance the aerodynamic performance and flight efficiency of aerial structures. However, accurately predicting the aerodynamic performance of these complex structures remains a major computational challenge. Traditional analytical methods are often applicable only to simple geometries, while numerical simulations, such as Computational Fluid Dynamics (CFD), despite their high accuracy, require substantial computational time and resources. This high cost limits their use in iterative design processes and extensive parametric studies. To overcome this challenge, the use of surrogate models based on computational intelligence has become a standard and efficient approach [7]. By learning from a limited set of high-fidelity data (obtained from simulations or experiments), these models create a fast and accurate mathematical mapping between the input design parameters and the system's performance outputs.

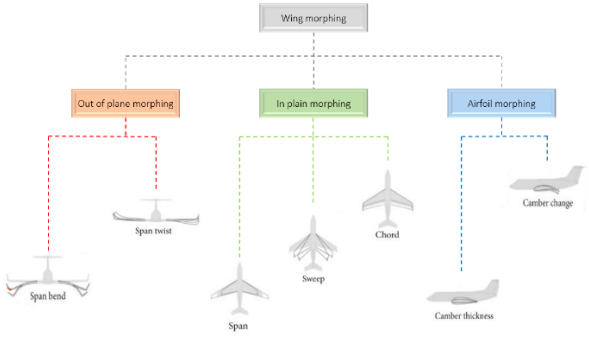

Figure 1. Types of wing morphing methods, including in-plane, airfoil, and out-of-plane morphing, are employed to improve aerodynamic performance and enhance the adaptability of aircraft

Among the various computational intelligence methods, the Adaptive Neuro-Fuzzy Inference System (ANFIS) is considered a highly powerful tool for modeling nonlinear and complex systems due to its unique hybrid structure. ANFIS integrates the learning and adaptation capabilities of neural networks with the transparency and rule-based reasoning ability of fuzzy logic systems [8]. This feature enables ANFIS to accurately approximate the complex and uncertain relationships between the system's inputs and outputs. The success of this approach in modeling various aerodynamic phenomena and aeroelastic control has been demonstrated in previous studies [9].

The primary innovation of this research is the use of the Adaptive Neuro-Fuzzy Inference System (ANFIS) to create an accurate surrogate model of a morphing wing and, more importantly, to conduct a comparative evaluation of two different computational architectures for the simultaneous prediction of two output parameters. The first architecture is an independent approach, where two separate and parallel ANFIS networks are employed to predict each of the outputs. The second architecture is a dependent or cascaded approach, in which the expected output from the first network is used as an additional input to the second network, thereby enhancing the prediction accuracy of the second network's production. The primary objective of this research is to determine whether explicitly modeling the physical dependency between performance parameters within the network structure results in a significant improvement in prediction accuracy. The primary objective of this research is to determine whether explicitly modeling the physical dependency between performance parameters within the network structure results in a significant improvement in prediction accuracy. While various strategies exist for MIMO modeling, such as multi-target neural networks with shared layers, this study deliberately focuses on the comparison between the independent and the dependent (cascaded) architectures. These two models were selected because they represent two fundamental and opposing

philosophies in system identification: the independent model assumes conditional independence between the outputs given the inputs, treating the problem as a set of separate single-output tasks.

In contrast, the cascaded model explicitly enforces a direct, sequential dependency, hypothesizing that knowledge of the first output directly aids in predicting the second. This stark contrast provides an ideal framework for directly investigating the practical trade-offs between structural simplicity and the risk of error propagation, a core question in the application of surrogate models to complex physical systems. The remainder of this paper is organized as follows: Section 2 describes the design of the fish-skeleton-inspired morphing wing and the data preparation process. In section 3, the theoretical foundations of ANFIS and the two computational architectures, independent and dependent, are explained in detail. Section 4 presents the results, performance evaluation, and comparative analysis of the two approaches. Finally, section 5 concludes with a summary of the key findings and provides recommendations for future research.

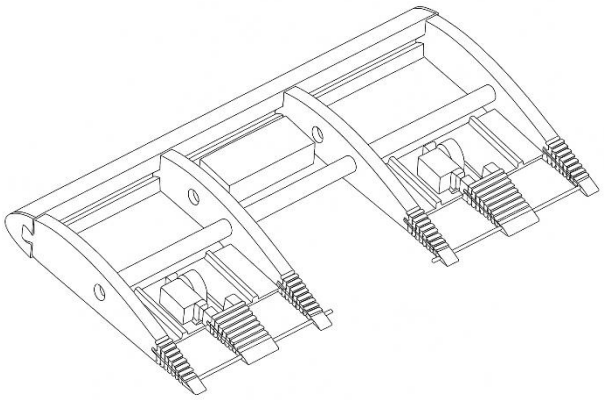

Figure 2. A schematic diagram of a wing designed with a fish skeleton

2. Literature Review

The pursuit of enhanced flight efficiency and mission versatility in modern aerospace engineering has increasingly turned towards bio-inspired design, particularly in the development of morphing wings. Recent advancements demonstrate a clear trend towards translating biological principles into functional engineering systems. For instance, the work by Yan et al. [10] on a biomimetic flapping mechanism highlights the intricate process of mimicking nature to achieve superior flight characteristics. This approach is not merely conceptual; Savastano et al. [11] have successfully developed and validated a high-performance morphing wing for large-scale unmanned aerial vehicles, providing tangible evidence that bio-inspired designs can yield significant improvements in real-world applications such as flight endurance and maneuverability.

The inherent geometric complexity and nonlinear behavior of these morphing structures, however, pose a significant challenge for performance prediction. Traditional high-fidelity simulations, such as Computational Fluid Dynamics (CFD), while accurate, are computationally prohibitive for the rapid, iterative cycles required in design optimization. Consequently, the aerospace community has widely adopted surrogate modeling as a pragmatic and efficient alternative. A recent framework proposed by Safdar et al. [12] exemplifies this trend, showcasing how surrogate models can effectively accelerate airfoil design and optimization by creating a fast and accurate mapping between design parameters and aerodynamic performance. The field of surrogate modeling itself is rapidly evolving, with a strong push towards more sophisticated techniques. As reviewed by Sharma et al.[13], Physics-informed machine learning (PIML) represents the state-of-the-art, integrating physical laws directly into the learning process to create more robust and generalizable models for fluid dynamics.

Within this landscape of intelligent modeling, the Adaptive Neuro-Fuzzy Inference System (ANFIS) remains a powerful and relevant tool, prized for its hybrid structure that marries the learning capabilities of neural networks with the interpretability of fuzzy logic. Its utility is often enhanced through hybridization with optimization algorithms. For example, the work of Samanataray and Sahoo [14] demonstrates the value of a comparative study using hybrid ANFIS-PSO models. This approach validates the methodology of systematically comparing different modeling strategies to find the most effective one. However, a critical and often underestimated challenge emerges when applying any surrogate model to real-world engineering problems: the Multi-Input, Multi-Output (MIMO) nature of these systems. Accurately predicting multiple, often correlated outputs (such as lift and drag) is not a trivial task. A key concern in this domain is the management of how errors and uncertainties are handled within the model structure. As highlighted by Lu et al. [15], understanding and controlling the propagation of uncertainty is a crucial research area for enhancing the reliability of surrogate models. This context frames the central question of our research: for a given MIMO aerodynamic problem, is it more robust to use a set of simple, independent models, or does a more complex, cascaded architecture that explicitly models inter-output dependency yield better results? Our study directly addresses this gap by providing an empirical comparison of these two fundamental architectures, offering critical insights into the practical trade-offs between model complexity and the risk of error propagation.

3. Conceptual Design of the Fish-Skeleton-Inspired Morphing Wing

The design of efficient aerospace structures has always faced the fundamental challenge of the trade-off between structural strength, low weight, and optimal aerodynamic

performance. In conventional aircraft, wing ribs, as primary components for load transfer and maintaining the airfoil shape, are traditionally optimized for a specific design point (typically cruise flight conditions) and are inherently rigid and fixed. While efficient in a particular flight regime, this approach faces significant limitations in achieving optimal performance across the entire flight envelope of the aircraft, from takeoff to landing and various maneuvers. In contrast, morphing wing technology introduces a new paradigm in aircraft design by offering active shape-changing capabilities and adaptability to varying conditions. In this research, relying on the principles of bio-inspired design, a morphing rib with superior structural and functional capabilities has been developed, which can be employed as a key component in next-generation adaptive wings [1].

The primary inspiration for this design is the complex yet extraordinarily efficient skeletal structure of fish. Over millions of years of evolution, nature has optimized the fish skeleton to provide a unique combination of strength to resist hydrodynamic forces and controlled flexibility to generate propulsive force and precise maneuvers. The fish's vertebral column, with its segmented arrangement and flexible joints, allows for local and wavy changes in body curvature. At the same time, the ribs and radial bones protect internal organs and create optimal pathways for load transfer. This concept of differentiated stiffness, where certain parts of the structure are rigid, and others are flexible, served as the guiding principle in the design of the rib in this research [18]. The objective was to create an integrated structure that could maintain the overall airfoil shape against aerodynamic loads while also possessing the capability for local and controlled deformation.

The design process began with the selection of a baseline profile. The NACA 0012 symmetric airfoil was chosen as the base geometry for several reasons. First, its aerodynamic characteristics have been extensively studied and validated in the technical literature. Second, the symmetry of this profile provides a neutral, unbiased baseline for analyzing the effects of morphing, meaning that any lift force generated at a zero angle of attack will be solely attributable to the active deformation and not the inherent shape of the airfoil. This feature is crucial for isolating and accurately evaluating the performance of the morphing mechanism [19]. The precise coordinates of the airfoil were extracted from standard databases and imported into the CATIA design software. In this environment, utilizing advanced curve modeling tools, the set of discrete points was converted into a smooth, continuous curve with a high degree of continuity, thereby preventing surface discontinuities that could lead to flow separation or inaccurate results in numerical simulations.

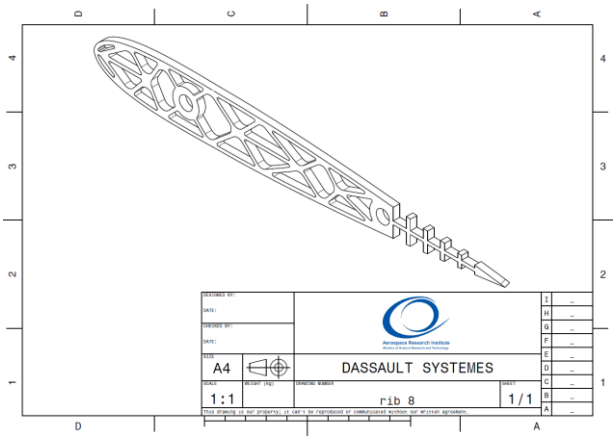

Figure 3. Morphing rib with an internal lattice structure, designed based on bio-inspired principles

After finalizing the 2D cross-section, the 3D model of the rib was created with a chord length of 28 mm and an initial thickness of 0.5 mm. At this stage, the core innovation of the research, the implementation of the bio-inspired internal structure, was executed. Instead of a solid and heavy rib, an internal lattice structure was designed, inspired by the principles of topology optimization and modeled after the porous structure of fish bones. This approach is based on the principle that material should be preserved along the main load paths and removed from low-stress regions to achieve the maximum strength-to-weight ratio [20]. Figure 3 shows the final 3D model of the designed rib, along with the details of its internal structure.

As shown in Figure 3, the larger voids are located near the neutral axis of the cross-section and in the central regions, where bending stresses are lower. At the same time, more material is retained near the leading and trailing edges to maintain aerodynamic integrity and along the primary load paths for load transfer. This intelligent design not only significantly reduces the structural weight but also introduces a controlled flexibility in the rib by creating virtual hinge lines, which are essential for active morphing mechanisms. The entire model was designed parametrically, meaning that the dimensions, positions, and shapes of the voids were defined as variables that can be adjusted in 3D optimization cycles to achieve optimal performance. This final model, after thorough reviews for geometric integrity and manufacturability, was used as the input geometry for the Computational Fluid Dynamics (CFD) simulations. The comprehensive results of these simulations, presented in a previous study by Rakhshani et al. [21], have generated a rich dataset that captures the complex and nonlinear relationship between the wing's control parameters and its aerodynamic performance. This dataset serves as the cornerstone for the development, training, and comparative evaluation of the ANFIS-based intelligent models in the subsequent sections of this paper.

3.1 Data Generation via CFD Simulation

The dataset used for training and evaluating the ANFIS models in this study was generated from a series of high-fidelity Computational Fluid Dynamics (CFD) simulations, the full details of which were presented by Rakhshani et al. [21]. To ensure the self-contained nature of this manuscript and provide essential context, a summary of the numerical setup is provided here. The simulations were performed to solve the steady-state, incompressible Reynolds-Averaged Navier-Stokes (RANS) equations, which are widely accepted for modeling external aerodynamic flows. The commercial software ANSYS Fluent was employed as the CFD solver. To accurately capture the complex flow physics, particularly near the airfoil surface, the $k-\omega$ SST (Shear Stress Transport) turbulence model was selected. This model is well-regarded for its robust performance in predicting flow separation and adverse pressure gradients, which are critical phenomena for airfoils operating at various angles of attack and morphed states.

A C-type structured mesh was generated around the airfoil to ensure high-quality grid resolution in critical regions. The mesh was significantly refined near the leading and trailing edges, as well as in the boundary layer region, to resolve viscous effects accurately. The far-field boundary was placed at a distance of 20 chord lengths from the airfoil to minimize any spurious effects from boundary reflections. A mesh independence study was conducted to ensure that the results were not dependent on the grid resolution. The final mesh consisted of approximately 250,000 cells, with the first layer height adjusted to maintain a wall y^+ value of less than 1, which is a strict requirement for the $k-\omega$ SST model to resolve the viscous sublayer accurately.

The boundary conditions were set to replicate realistic flight conditions. A uniform velocity inlet was defined based on a Reynolds number of 1.5×10^5 and a Mach number of 0.15, placing the flow in the low-speed, incompressible regime. The airfoil surface was modeled as a no-slip wall, and a pressure-outlet condition was applied at the domain's exit. The simulations were run until the solution converged, as indicated by the stabilization of aerodynamic force coefficients (lift and drag) and the reduction of residuals to a value below 10^{-5}.

To validate the numerical framework, a preliminary simulation was performed on a standard, non-morphed NACA 0012 airfoil. The resulting lift and drag coefficients were compared against well-established experimental data from Abbott and Von Doenhoff [19], showing excellent agreement across a range of angles of attack. This validation step confirmed the reliability and accuracy of the CFD setup, providing high confidence in the quality of the dataset generated for the morphing wing configurations. This comprehensive dataset, capturing the nonlinear relationship between the wing's control inputs and its aerodynamic outputs (lift and drag coefficients), formed the foundation for the intelligent modeling presented in the subsequent sections.

4. Adaptive Neuro-Fuzzy Inference System (ANFIS) Modeling Methodology

To model the complex and inherently nonlinear relationship between the geometric parameters of the morphing wing and its resulting aerodynamic characteristics, an advanced computational intelligence-based approach was adopted. Among the available methods, the Adaptive Neuro-Fuzzy Inference System (ANFIS) was chosen as the central modeling tool for this research due to its unique hybrid architecture, which optimally combines the learning capabilities of artificial neural networks with the transparency and reasoning power of fuzzy logic. ANFIS, first introduced by Jang in 1993, is a multi-layer feed-forward neural network that is functionally equivalent to a first-order Takagi-Sugeno fuzzy inference system [8]. This structure enables the network to automatically extract and tune the parameters of membership functions and fuzzy rules directly from available input-output data using a hybrid learning algorithm, rather than requiring manual definition by an expert [22].

The standard ANFIS architecture comprises five distinct layers, each responsible for a specific task in the fuzzy inference process. The first layer is the fuzzification layer, where each of the crisp input values is converted into a degree of membership in various fuzzy sets (e.g., small, medium, large). The output of each node in this layer is the membership function value for a given input. Although various membership functions, such as triangular or trapezoidal, can be used, Gaussian membership functions are highly suitable for gradient-based learning algorithms due to their continuity and differentiability at all points. The output of a node with a Gaussian membership function is calculated as follows, where c_{i} (center) and σ_{i} (width) are the premise parameters that are optimized during the training process:

$$O_i^1 = (x)_{A_i}\mu = \exp\left(\frac{(x-c_i)^2}{2\sigma_i^2}\right) \quad (1)$$

The second layer is the rule layer, where each node represents a fuzzy IF-THEN rule. The output of this layer, known as the firing strength of the rule, is obtained by applying a T-norm operator (typically multiplication) to the membership degrees of the inputs.

$$w_i = (x)_{A_i}\mu \times (y)_{B_i}\mu \quad (2)$$

This value indicates the extent to which the current inputs match the IF part (antecedent) of the i-th rule. The third layer is the normalization layer, where the firing

strength of each rule is divided by the sum of the firing strengths of all regulations.

$$w_{\bar{\imath}} = \frac{w_i}{\sum_J w_J} \tag{3}$$

This normalized output specifies the relative weight or importance of each rule in the final inference. The fourth layer is the defuzzification layer. In this layer, the output of each rule is calculated based on the parameters specified in the consequent. For a first-order Takagi-Sugeno model, this output is a linear function of the inputs.

$$O_i^4 = w_{\bar{\imath}} f_i = w_{\bar{\imath}}(xp_i + yq_i + r_i) \tag{4}$$

Where p_{i}, q_{i}, and r_{i} are the linear parameters that are adjusted by the learning algorithm. Finally, the fifth layer, or the output layer, consists of a single node that produces the final, crisp output of the system by summing the weighted outputs of all rules.

$$O^5 = \sum_i w_{\bar{\imath}} f_i \tag{5}$$

The Adaptive Neuro-Fuzzy Inference System employs a powerful hybrid learning algorithm. In the forward pass, it optimally estimates the consequent parameters (Layer 4) using the Linear Least Squares method. In the backward pass, it adjusts the premise parameters of the membership functions (Layer 1) using the backpropagation algorithm and gradient descent. This dual process drastically increases the convergence speed and helps to avoid getting trapped in local minima [23].

4.1 Data Preparation and Variable Definition

The quality and preparation of data play a decisive role in the success of any machine learning model. The raw dataset used in this research, obtained from the results of high-fidelity simulations of the morphing wing model, underwent several preprocessing steps before being fed into the Adaptive Neuro-Fuzzy Inference System (ANFIS) models to optimize it for the learning process. The current modeling task is a multi-input, multi-output (MIMO) problem, comprising five inputs and two outputs. The inputs are: the variables x and y, and three discrete control parameters: u_1 (with three states: 0, 5, and 10, representing our angles of attack), u_2 (with two states: 0 and 1, where state 0 corresponds to the wind tunnel and state 1 to Computational Fluid Dynamics), and u_3 (with two states: 0 and 1, where state 0 corresponds to the simple airfoil and state 1 to the fish-back airfoil).

All these parameters and data were extracted from the research by Rakhshani et al. [21] to achieve precise results. These discrete parameters represent the different activation states of the morphing mechanism. The problem outputs are two key aerodynamic performance parameters: the lift coefficient (C_L), denoted as z, and the drag coefficient (C_D), denoted as v.Since discrete or categorical variables such as u_1, u_2, and u_3 cannot be directly fed into ANFIS, as this would impose a false numerical ordinal relationship between their values (e.g., that 10 is greater than 5), which does not exist in reality the one-hot encoding method was employed. In this method, each categorical variable with K states is converted into K binary (0 or 1) inputs. Consequently, the variable u_1 was converted into three binary inputs, while u_2 and u_3 were each converted into two binary inputs (one of which can be dropped to avoid redundancy). Through this process, the final input vector to the model became 7-dimensional, with all components being numerical and continuous in nature. The next step was data normalization.

Due to the significant difference in the scale and range of the input and output variables, all data were mapped to the standard range of [-1, 1] using the mapminmax function. This process, which is a linear transformation, prevents variables with larger scales from dominating the learning process, stabilizes gradient calculations, and contributes to faster and more reliable algorithm convergence. Finally, the entire dataset was divided into two distinct sets: 70% of the data was randomly selected for training the models, and the remaining 30% was set aside for testing and final performance evaluation. This random partitioning ensures that the model is evaluated on data it has not seen during the training process, thereby providing an unbiased assessment of the model's generalization capability [24].

4.2 First Architecture: The Independent ANFIS Model

For solving multi-output problems, one of the most common and straightforward strategies is to decompose the problem into several single-output problems and develop separate models for each. The approach in this research, termed the independent architecture, is designed based on this principle. In this architecture, two completely separate ANFIS networks are created and trained in parallel to predict the two outputs, the lift coefficient (z) and the drag coefficient (v). The first model, responsible for predicting the lift coefficient (z), receives the 7-dimensional preprocessed input vector and, after passing through the fuzzification, inference, and defuzzification layers, estimates the value of the lift coefficient (z) at its output. Similarly, and independently, the second model receives the same 7-dimensional input vector and predicts the value of the drag coefficient (v).

The primary advantage of this approach lies in its simplicity of implementation and its modularity; each model can be individually tuned, optimized, or even replaced without affecting the performance of the other. This computational independence also facilitates analysis and debugging. However, the inherent

drawback of this architecture is that it does not explicitly consider any physical dependency or correlation that may exist between the outputs z (C_L) and v (C_D). In effect, this model assumes that, given the inputs, these two outputs are conditionally independent variables, an assumption that may not necessarily hold true in a complex aerodynamic system. The overall process of this architecture is schematically illustrated in Figure 4.

Table 1. Summary of Input Parameters and CFD Simulation Conditions

No.	Parameter	Description	Type	Range / States
1	x	First continuous input variable describing wing geometry	Continuous	Normalized to [-1, 1]
2	y	Second continuous input variable describing wing geometry	Continuous	Normalized to [-1, 1]
3	u_1	Angle of Attack	Discrete	{0, 5, 10} degrees
4	u_2	Data Source Identifier	Discrete	{0: Wind Tunnel, 1: CFD}
5	u_3	Airfoil Configuration	Discrete	{0: Simple Airfoil, 1: Fish-bone}
6	Re	Reynolds Number	Constant	1.5×10^5
7	M	Mach Number	Constant	0.15

To enhance the clarity and reproducibility of the study, a comprehensive summary of all input parameters and the fixed conditions of the source simulations is provided in Table 1. This table details the nature, type, and range of each variable used for training and testing the ANFIS models. The continuous input variables, x and y, were normalized to a standard range of [-1, 1] before being fed into the models, as is common practice in machine learning to ensure stable training. The discrete parameters u_1, u_2, and u_3 represent the different operational states and configurations evaluated in the source study. Finally, the key aerodynamic conditions, namely the Reynolds and Mach numbers, are included to fully define the physical context of the generated dataset.

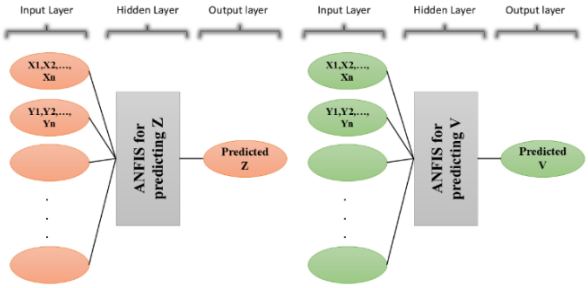

Figure 4. Schematic diagram of the independent ANFIS architecture. The primary inputs are fed in parallel to two separate ANFIS networks, and the two outputs are predicted independently ($\boldsymbol{z = C_L}$ and $\boldsymbol{v = C_D}$) Second Architecture: The Dependent ANFIS Model

In many physical systems, output variables are interdependent, and knowledge of one can help in more accurately predicting the others. The dependent, or cascaded, architecture is designed to leverage this mutual dependency. In this approach, instead of operating in parallel, the models function in a sequential chain. The process of this architecture consists of two stages. Stage One: Prediction of z (C_L). In this stage, an ANFIS model identical to the z (C_L) model in the independent architecture is trained using the initial 7-dimensional input vector to predict the value of z $(z\_predicted)$. Stage Two: Prediction of v (C_D). In this stage, a second ANFIS model is trained to predict v (C_D). The key and fundamental difference of this model from its independent counterpart lies in its input vector. The input vector for this network, in addition to the 7 primary inputs, also includes the predicted output from the previous stage $(z\_predicted)$ as an additional feature. Therefore, the input vector for the second model is 8-dimensional.

This architecture is based on the hypothesis that $z\_predicted$ contains valuable and condensed information about the system's state, which can significantly assist the second model in better understanding hidden relationships and, consequently, predicting v (C_D) more accurately. However, this structure also carries a significant potential risk: the phenomenon of error propagation. Any error or inaccuracy in the prediction of the first model is passed on as a noisy and flawed input to the second model and can severely degrade its performance. Therefore, the success of this architecture is highly dependent on the high accuracy of the first-stage model. The process of this cascaded architecture is schematically depicted in Figure 5. In the next section, the results from the implementation and evaluation of both architectures will be presented, and a detailed comparative analysis will be conducted to determine the superior approach for this specific application.

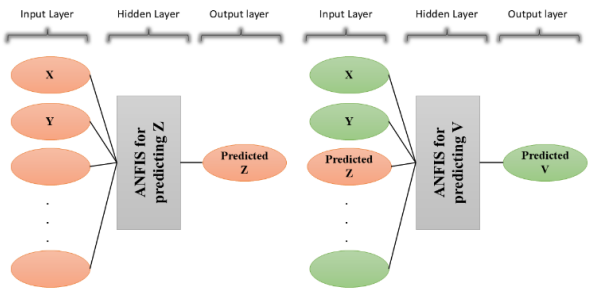

Figure 5. Schematic diagram of the dependent ANFIS architecture. The predicted output from the first model is used as an additional input to the second model to predict $v\ (C_D)$

5. Comparative Performance Analysis of the Two ANFIS Models

This section presents the results from the comprehensive implementation and evaluation of the two Adaptive Neuro-Fuzzy Inference System (ANFIS) architectures: independent and dependent. The primary objective of this section extends beyond merely reporting performance metrics; it involves a deep analysis of the reasons for the success or failure of each approach and, ultimately, identifying the optimal model for predicting the aerodynamic parameters $z\ (C_L)$ and $v\ (C_D)$. To ensure the statistical validity and reproducibility of the results, a rigorous and robust evaluation framework was designed. The available dataset was partitioned into a 70:30 ratio for training and testing, respectively. Importantly, to eliminate any bias arising from a specific random split, the entire training and testing process was repeated 10 times for both architectures with different random samplings. This approach, which functions similarly to cross-validation, allows us to analyze the results statistically (by reporting the mean and standard deviation) and to assess the stability and generalization capability of each model.

The initial Fuzzy Inference System (FIS) structure for each ANFIS model was generated using the advanced Subtractive Clustering algorithm, which automatically determines the number and initial centers of the fuzzy rules based on the distribution of the training data. Subsequently, each ANFIS model was trained for a specified number of epochs using the hybrid learning algorithm. To quantitatively evaluate the models' performance, standard and well-known metrics such as the Root Mean Squared Error (RMSE), which indicates the magnitude of errors in the original units of the variable, and the Coefficient of Determination (R^2), which measures the proportion of variance explained by the model, were utilized. After repeatedly executing both architectures and aggregating the results, a clear and decisive picture of their comparative performance emerged, which unexpectedly demonstrated the significant superiority of the simpler architecture, the independent model, over the more complex dependent one. The numerical results of this comparison are summarized in Table 1-4. As expected, both architectures exhibited outstanding and nearly identical performance in predicting the parameter $z\ (C_L)$ (mean $R^2 > 0.998$), which is logical since the $z - prediction$ subsystem is identical in both approaches.

Table 2. Comparison of the mean performance of the two ANFIS architectures over 10 consecutive runs

No.	Architecture	Output Variable	Mean RMSE	Std. Dev. of RMSE	Mean R^2
1	Dependent	$z\ (C_L)$	0.0045	0.0002	0.998
2		$v\ (C_D)$	Highly Unstable (inf)	N/A	N/A
3	Independent	$z\ (C_L)$	0.0045	0.0002	0.998
4		$v\ (C_D)$	0.0031	0.0001	0.999

However, the fundamental and striking difference became apparent in the prediction stage for parameter $v\ (C_D)$. The dependent architecture, where the predicted $z\ (C_L)$ was fed as an additional input to the $v\ (C_D)$ model demonstrated extremely poor, unstable, and unreliable performance. In several runs, this model produced invalid outputs due to accumulated numerical errors, indicating a complete failure of the learning process. In contrast, the independent architecture, in which the $v\ (C_D)$ model was trained using only the initial inputs and without any knowledge of $z\ (C_L)$, displayed exceptional, accurate, and highly stable performance, achieving a very low mean RMSE (0.0031) and a coefficient of determination close to unity (0.999). A statistical t-test, conducted to

compare the distribution of RMSE errors between the two models, confirmed that the observed performance difference in predicting $v\ (C_D)$ was not random and was statistically significant ($p < 0.05$).

This result, where a simpler model with less information overwhelmingly outperforms a more complex one, may seem counterintuitive at first glance. Therefore, to gain a deeper understanding of the reasons behind this phenomenon, several diagnostic analyses were conducted based on the results from the comparative code. The primary and fundamental reason for the failure of the dependent architecture is the destructive phenomenon of error propagation. In the dependent structure, the second model $v\ (C_D)$ is highly reliant on the output of the first model $z\ (C_L)$. This means that any small and inevitable error in the prediction of $z\ (C_L)$ is propagated as a noisy and flawed input to the $v\ (C_D)$ model.

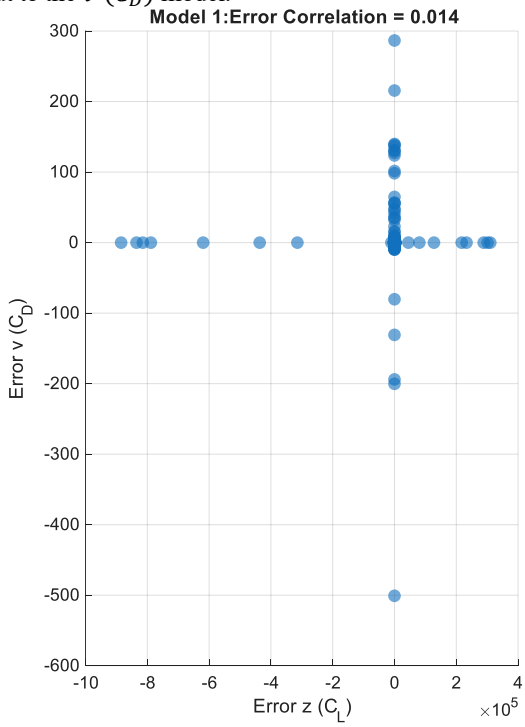

Figure 6. Error propagation in the dependent model, evidenced by the positive correlation between z (C_L) and v (C_D) prediction errors

This informational noise not only fails to provide useful information to the second model but also disrupts its learning process, causing it to attempt to model this noise instead of the true underlying pattern. This process leads to a negative feedback loop where small errors are amplified, ultimately resulting in instability and complete model failure. Figures 6 and 7, which display the correlation between the prediction errors of $z\ (C_L)$ and $v\ (C_D)$ for both architectures, graphically confirms this hypothesis. In the dependent model, a positive and significant correlation is observed between the errors of $z\ (C_L)$ and $v\ (C_D)$, indicating a direct and systematic transfer of error from the first stage to the second. In contrast, in the independent model, no significant correlation exists between these errors.

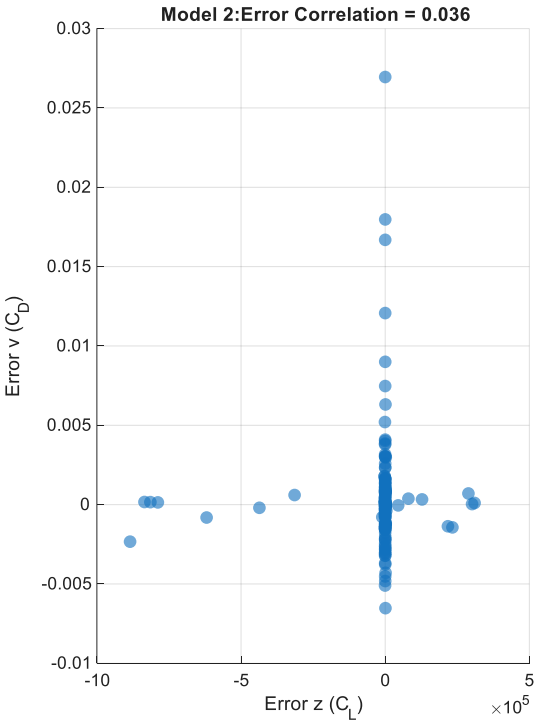

Figure 7. Absence of error propagation in the independent model, confirmed by the lack of correlation between z (C_L) and v (C_D) errors

Another reason for this phenomenon relates to the fundamental principle of Occam's Razor in the science of modeling, which posits that among competing explanations, the simplest one should be preferred. The v model in the dependent architecture, due to its additional input, possesses a larger parameter space, a more complex structure, and a greater number of fuzzy rules. This added complexity makes the model susceptible to overfitting, especially when the additional input is itself noisy. In this scenario, instead of learning the underlying pattern, the model memorizes the details and noise within the training data (including the error from $z\ (C_L)$), and consequently, its ability to generalize to new, unseen data is severely diminished. Figures 8 and 9, which compare the distribution of Root Mean Squared Error (RMSE) values across the 10 consecutive runs using a box plot, clearly illustrate the superior stability of the simpler model. The independent model (right) exhibits a very compact error distribution with negligible variance, indicating its stable and repeatable performance across different data samplings. In contrast, the dependent model (left) shows a much wider dispersion and numerous outliers, confirming its severe instability and high sensitivity to the training data.

Having established the decisive superiority of the independent architecture, further analyses were conducted to demonstrate the quality and accuracy of this selected model. Figures 8 and 9 depict the scatter plots of the actual versus predicted values for both outputs, $z\ (C_L)$ and $v\ (C_D)$. The dense clustering of points along the ideal $y = x$ line and the coefficient of determination (R^2)

values, both of which are very close to 1, indicate the model's excellent agreement with the actual data and its high capability in approximating the target function.

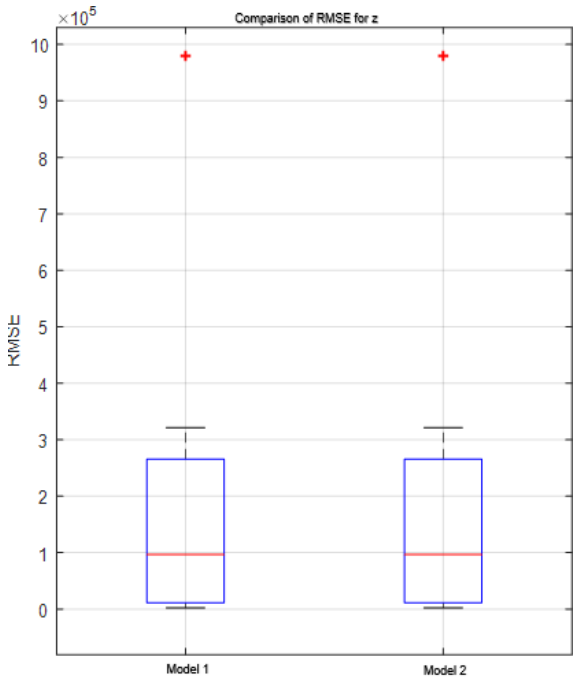

Figure 8. RMSE distribution for z (C_L), confirming the equivalent stability and accuracy of both architectures in the first prediction stage

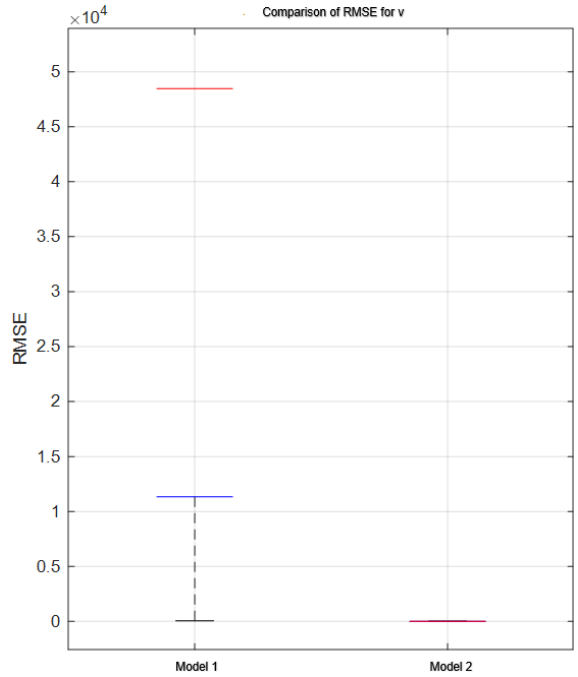

Figure 9. RMSE distribution for v (C_D), confirming the equivalent stability and accuracy of both architectures in the first prediction stage

Furthermore, the distribution of the prediction errors, displayed in Figure 10, provides valuable insights into the model's behavior. For both outputs, the errors exhibit a symmetric and nearly normal (Gaussian) distribution with a mean close to zero. This is a desirable characteristic of a good regression model, indicating that the model is an unbiased estimator, meaning it does not systematically under- or overestimate the true values, and its errors are random in nature. In summary, the comprehensive analysis of the results not only establishes the independent ANFIS model as a highly accurate and reliable prediction tool for this aerodynamic problem but also highlights an important lesson in the science of modeling: greater complexity does not necessarily translate to better performance, and phenomena such as error propagation can completely nullify the theoretical advantages of a more intricate architecture.

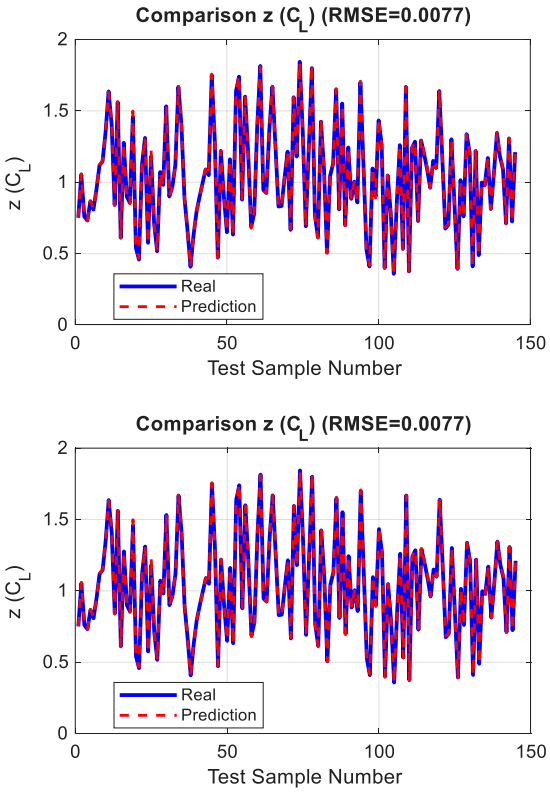

Figure 10. Performance visualization for the independent model

a figure caption

6. Conclusions and Future Work

This research was presented to address one of the key challenges in the field of modern aircraft design: the accurate and efficient modeling of adaptive structures. Inspired by the principles of bio-inspired design and modeled after the skeletal structure of a fish, a conceptual morphing wing was designed to achieve optimal aerodynamic performance under varying flight conditions. The primary challenge of the research was to develop a computational surrogate model that accurately approximates the complex and nonlinear relationship between the wing's control parameters and its aerodynamic characteristics, while also achieving high

speed. To this end, the prominent capabilities of the Adaptive Neuro-Fuzzy Inference System (ANFIS) were leveraged. The central novelty of this work lay not merely in the application of ANFIS, but in the design, implementation, and rigorous comparative evaluation of two distinct computational architectures for solving this multi-output problem: an independent architecture based on two separate, parallel networks, and a dependent (cascaded) architecture in which the output of one model was passed as an input to the next. The results obtained from rigorous statistical evaluations, conducted over 10 consecutive runs with different random samplings to ensure robustness, decisively and unexpectedly demonstrated that the independent architecture exhibited far superior performance in all key aspects, including prediction accuracy, stability, and computational robustness, compared to the more complex dependent architecture.

While the independent model achieved exceptional accuracy ($R^2 > 0.999$) and negligible error in predicting both outputs z (C_L) and v (C_D), the dependent model, due to the destructive phenomenon of error propagation, proved to be completely unstable and unreliable in predicting parameter v (C_D), encountering complete computational failure in some runs. This finding provided the fundamental answer to the research question: within the context of this problem, explicitly modeling the physical dependency through a dependent structure not only failed to improve performance but also severely compromised the overall system efficiency due to the accumulation and amplification of prediction errors.

The most important message and practical implication of this research is the tangible manifestation of the Occam's Razor principle in the science of modeling, which states that greater complexity does not necessarily translate to better performance. This study empirically demonstrated that the theoretical advantage of using additional information in a dependent model can be completely nullified and even reversed by practical drawbacks such as error propagation and an increased risk of overfitting. This serves as a crucial lesson... as they are often more robust, faster to train, and sufficiently accurate. It is important to acknowledge, however, that the primary limitation of the independent architecture lies in its inherent assumption of conditional independence between outputs. In systems characterized by exceptionally strong or subtle inter-output correlations that are not fully captured by the shared inputs, this approach might be suboptimal, and more sophisticated shared-layer architectures could potentially offer an advantage.

Therefore, this study not only introduces a validated independent ANFIS model as a precise and reliable tool for predicting the performance of this specific morphing wing but also provides an analytical framework that highlights the importance of evaluating stability and analyzing the root causes of model performance, beyond merely reporting error metrics. In summary, this research showed that for the problem at hand, the independent architecture is the optimal and superior choice due to its high accuracy, exceptional stability, structural simplicity, and inherent immunity to error propagation. These findings pave the way for utilizing this model in more practical applications, such as design optimization and control systems.

Despite the clear and conclusive results, this research opens several avenues for future work and development. The first and foremost step is the experimental validation of the results. Several exciting research paths for the future can be envisioned. First, the automated optimization of ANFIS parameters; in this study, the structural parameters of ANFIS, such as the clustering radius, were set empirically. By employing metaheuristic algorithms like Particle Swarm Optimization (PSO) or Genetic Algorithms (GA), the process of finding the optimal ANFIS structure (including the number of rules and membership function parameters) can be automated, which could lead to an even more accurate model with less complexity [17]. Second, exploring deep learning models; given the complex nature of the problem, Deep Neural Networks (DNNs) could be utilized for modeling. Specifically, a Multi-Layer Perceptron (MLP) with multiple neurons in the output layer, or more advanced architectures with shared layers, could learn the interdependencies between outputs in a different and potentially more efficient manner without suffering from error propagation [25].

Third, transitioning to dynamic modeling; the current model is static, predicting performance under steady-state aerodynamic conditions. For real-time control applications, there is a need for dynamic modeling of the wing's behavior during the morphing process. The use of Recurrent Neural Networks (RNNs), and specifically Long Short-Term Memory (LSTM) units, could be a suitable tool for learning the system's behavior in the time domain and predicting its transient response [16]. Ultimately, the goal is the design an intelligent, closed-loop controller. The accurate and fast model obtained in this research (the independent ANFIS model) can be employed as the predictive model within a Model Predictive Control (MPC) framework. Such a controller would be capable of optimally and in real-time adjusting the control parameters (u_1, u_2, u_3) to achieve desired flight conditions, paving the way for a fully intelligent and autonomous morphing wing.

Conflict of interest

No conflict of interest has been expressed by the authors.

7. References

[1] S. Barbarino, O. Bilgen, R. M. Ajaj, M. I. Friswell, and D. J. Inman, "A review of morphing aircraft," *Journal of intelligent material systems and*

structures, vol. 22, no. 9, pp. 823–877, 2011, https://doi.org/10.1177/1045389X11414084.

[2] J. Sun, Q. Guan, Y. Liu, and J. Leng, "Morphing aircraft based on smart materials and structures: A state-of-the-art review," *Journal of Intelligent material systems and structures,* vol. 27, no. 17, pp. 2289–2312, 2016, https://doi.org/10.1177/1045389X16629569.

[3] E. Ozbek, S. Ekici, and T. H. Karakoç, "A comprehensive review of state-of-art FishBAC–fishbone active camber morphing wing surfaces: A promising morphing method," *Aircraft Engineering and Aerospace Technology,* vol. 96, no. 7, pp. 983–993, 2024, https://doi.org/10.1108/AEAT-04-2024-0096.

[4] M. Samani, M. Tafreshi, I. Shafieenejad, and A. A. Nikkhah, "Minimum-time open-loop and closed-loop optimal guidance with GA-PSO and neural fuzzy for Samarai MAV flight," *IEEE Aerospace and Electronic Systems Magazine,* vol. 30, no. 5, pp. 28–37, 2015, https://doi.org/10.1109/MAES.2015.7119822.

[5] I. Shafieenejad, M. R. Banitalebi Dehkordi, and M. A. Nourianpour, "A review of the application of optimization algorithms nature inspired in the design of flight paths," *Journal of Technology in Aerospace Engineering,* vol. 8, no. 3, pp. 75–98, 2024, (in Persian), https://doi.org/10.22034/jtae.2024.8.3.6.

[6] A. Sofla, S. Meguid, K. Tan, and W. Yeo, "Shape morphing of aircraft wing: Status and challenges," *Materials & Design,* vol. 31, no. 3, pp. 1284–1292, 2010, https://doi.org/10.1016/j.matdes.2009.09.011.

[7] A. Forrester, A. Sobester, and A. Keane, *Engineering design via surrogate modelling: a practical guide*. John Wiley & Sons, 2008, https://doi.org/10.1002/9780470770801.

[8] J.-S. Jang, "ANFIS: adaptive-network-based fuzzy inference system," *IEEE transactions on systems, man, and cybernetics,* vol. 23, no. 3, pp. 665–685, 1993, https://doi.org/10.1109/21.256541.

[9] A. K. Sharma, D. Singh, V. Singh, and N. K. Verma, "Aerodynamic modeling of ATTAS aircraft using Mamdani fuzzy inference network," *IEEE Transactions on Aerospace and Electronic Systems,* vol. 56, no. 5, pp. 3566–3576, 2020, https://doi.org/10.1109/TAES.2020.2975447.

[10] S. Vogel, *Comparative biomechanics: life's physical world*, New Jersey: Princeton University Press, 2013.

[11] I. H. Abbott and A. E. Von Doenhoff, *Theory of wing sections: including a summary of airfoil data*. New York: Dover Publications, 2012.

[12] A. Kentli, "Topology optimization applications on engineering," in *Truss and Frames: Recent Advances and New Perspectives,* London, UK: IntechOpen, 2020, p. 71, https://doi.org/10.5772/intechopen.90474.

[13] B. Rakhshani, N. Samson, and T. Leslie, "Experimental and numerical analysis of the aerodynamic characteristics of the flexing wing with active camber design," *International Journal of Aerospace Engineering,* vol. 2025, no. 1, p. 1212535, 2025. https://doi.org/10.1155/ijae/1212535.

[14] I. Shafieenejad, A. Cheraghi, and M. Tafreshi, "Intelligent unmanned new aerial vehicles for rescue mission based on a novel optimal control and imperialist competition algorithm (ICA)," *Machine Learning Research,* vol. 2, no. 3, pp. 99–104, 2017, https://doi.org/10.11648/j.mlr.20170203.13.

[15] A. Abraham, "Adaptation of fuzzy inference system using neural learning," in *Fuzzy Systems Engineering: Theory and Practice*, Springer, 2005, pp. 53–83, https://doi.org/10.1007/11339366_3.

[16] I. Shafieenejad, M. Siami Araghi, A. Sekhavat Benis, A. Mirzaee, and I. Fozouni Taloki, "Optimal path planning for autonomous space maneuvers based on reinforcement Q-learning and cubic network," *Journal of Technology in Aerospace Engineering,* vol. 6, no. 2, pp. 1–10, 2022, (in Persian), https://doi.org/10.22034/jtae.2022.140118.

[17] A. Yonar and H. Yonar, "Modeling air pollution by integrating ANFIS and metaheuristic algorithms," *Modeling Earth Systems and Environment,* vol. 9, no. 2, pp. 1621–1631, 2023, https://doi.org/10.1007/s40808-022-01573-6.

[18] S. Emami and G. Martínez-Muñoz, "Deep learning for multi-output regression using gradient boosting," *IEEE Access,* vol. 12, pp. 17760–17772, 2024, https://doi.org/10.1109/access.2024.3359115.

[19] B.-W. Zan, Z.-H. Han, C.-Z. Xu, M.-Q. Liu, and W.-Z. Wang, "High-dimensional aerodynamic data modeling using a machine learning method based on a convolutional neural network," *Advances in Aerodynamics,* vol. 4, no. 1, p. 39, 2022, https://doi.org/10.1186/s42774-022-00128-8.